Hindawi Publishing Corporation
Advances in Materials Science and Engineering
Volume 2016, Article ID 1016482, 9 pages
http://dx.doi.org/10.1155/2016/1016482

Research Article

Crack-Depth Prediction in Steel Based on Cooling Rate

M. Rodríguez-Martín,[1,2] S. Lagüela,[1,3] D. González-Aguilera,[1] and P. Rodríguez-Gonzálvez[1]

[1]*Department of Cartographic and Terrain Engineering, University of Salamanca, Polytechnic School of Avila, Hornos Caleros 50, 05003 Ávila, Spain*
[2]*Faculty of Sciences and Arts, Catholic University of Avila (UCAV), C/Canteros s/n, 05005 Ávila, Spain*
[3]*Applied Geotechnologies Research Group, University of Vigo, Campus Lagoas-Marcosende, Rúa Maxwell s/n, 36310 Vigo, Spain*

Correspondence should be addressed to M. Rodríguez-Martín; ingmanuel@usal.es

Received 14 September 2015; Accepted 13 January 2016

Academic Editor: Gianluca Percoco

One criterion for the evaluation of surface cracks in steel welds is to analyze the depth of the crack, because it is an effective indicator of its potential risk. This paper proposes a new methodology to obtain an accurate crack-depth prediction model based on the combination of infrared thermography and the 3D reconstruction procedure. In order to do this, a study of the cooling rate of the steel is implemented through active infrared thermography, allowing the study of the differential thermal behavior of the steel in the fissured zone with respect to the nonfissured zone. These cooling rate data are correlated with the real geometry of the crack, which is obtained with the 3D reconstruction of the welds through a macrophotogrammetric procedure. In this way, it is possible to analyze the correlation between cooling rate and depth through the different zones of the crack. The results of the study allow the establishment of an accurate predictive depth model which enables the study of the depth of the crack using only the cooling rate data. In this way, the remote measure of the depth of the surface steel crack based on thermography is possible.

1. Introduction

Welding is the most important joining process for metallic materials but is also an aggressive technique, taking into account the fact that an important heating process is applied in order to meld the material and that high thermomechanical stresses induced by the welding procedure could cause several security problems. Defects present in the material are harmful and dangerous for the integrity of the joints. The most commonly observed welding flaws include the following: lack of fusion, lack of penetration, gas holes, porosity, cracking process, and inclusions, which are all typified in the international quality standards [1]. Some types of defects may occur more frequently than others for a particular welding process. In order to maintain the desired level of structural integrity, welds must be inspected in accordance with the quality standards. The results of the inspection of welds also provide useful information to identify potential problems in the manufacturing process and to improve the welding operations [2]. In the current industry and building practice, welding inspection is the responsibility of inspectors certified according to international standards [3].

In these cases, the cracking process is critical because the quality of the result may influence the failure of an important structural element and, consequently, the full collapse of the structure with drastic consequences. Welds are the origin of structural feebleness in the majority of cases and should be systematically checked in order to ensure the structural integrity of the components. Therefore, establishing a detailed geometric study of the crack is really important, since the knowledge of the size of the crack (measures along surface and depth) presents enormous importance for the evaluation of materials. If the depth of the crack is not known, the rejection of the material will be automatic due to the impossibility of predicting its risk; else, if the depth of the crack is known, this information could be used to calculate the risk of maintaining the material and to assess the possibility of its rejection [4]. Thus, the possibility of measuring accurately the depth of small cracks is highly useful, since they represent the least dangerous factor and will therefore present a more likely

probability to be accepted without removal [5]. Moreover, the crack depth would increase with the crack propagation length [6].

The methods most frequently used for the measurement of surface cracks are ultrasounds [5] and radiography [7]. More novel and sophisticated methods are scanning cameras [8], laser [9], 2D stereoimaging [10], and macrophotogrammetry [11]. Among them, the only one that allows the complete dimensioning for crack depth is the radiographic method [7] although an approximation for the prediction of depth of the crack has been raised with thermography using absolute values of temperature [12].

Infrared Thermographic (IRT) methods have also been used in the welding field for the control and metallurgical characterization of the welding process through the study of emissivity [13]. IRT has been used to inspect and measure the adhering slag on the weld during the welding process [14]. Another important use of the thermographic methods is the inspection and evaluation of materials, mainly composite materials. However, their application to inspect steel welds is not as settled as the previous methods. Relevant research shows positive results, ensuring a promising future for the application of the technique in testing engineering. The most extended modality of thermography used to evaluate materials is the one denominated as *active thermography*, which is based on the study of the thermal reaction of the material when external signal stimulation is applied. The signal can be applied in different ways, such as heat pulses [15], one-frequency modulated signal, also known as lock-in method [16], mechanical vibrations [17], ultrasounds [18], and microwaves [19]. In this paper, authors apply a new approach to establish a protocol for the prediction of crack depth from cooling rate data. Cooling rate data are extracted for each pixel from a sequence of thermal images using an algorithm (*pixelwise algorithm for time derivative of temperature*) based on the experimental proposal of [20]. Cooling rate data are integrated with geometrical depth data extracted following the macrophotogrammetric procedure established for welding in [11]. The objective is to establish a prediction model that allows the estimation of depth of the crack using an IR camera and low-temperature long-pulsed heating/cooling of the metal.

This paper is organized as follows: after this introduction, Section 2 presents the equipment used and the testing methodology; Section 3 analyzes the results obtained and the information gathered from the combined thermographic and geometric knowledge of the defects detected with thermography. Last, Section 4 explains the conclusions drawn from the presented study.

2. Materials and Methods

The materials needed and the methods followed to implement the procedure are shown in this section.

2.1. Materials. A welded plaque of low carbon with a thickness of 7.5 mm was used as subject of the study, given the presence of a crack with a little notch in the face of weld (Figure 1).

Table 1: Parameters for the geometric calibration of the IR camera NEC TH9260.

Focal length (mm)	14.35 ± 0.44
Format size (mm)	5.98×4.50 (± 0.07)
Pixel size (mm)	$9.34 \cdot 10^{-3} \times 9.37 \cdot 10^{-3}$
Principal point (X_{PP}) (mm)	2.99 ± 0.07
Principal point (Y_{PP}) (mm)	2.28 ± 0.09
Lens distortion	
K_1	$-1.32 \cdot 10^{-2}$
K_2	$1.08 \cdot 10^{-3}$
P_1	$-3.43 \cdot 10^{-4}$
P_2	$1.44 \cdot 10^{-3}$

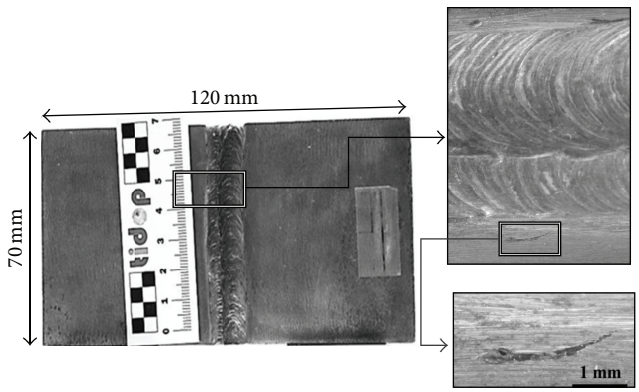

Figure 1: Low-carbon steel weld used as specimen. This presents a toe crack close to the limit of the weld (macroimage).

The plaque has been welded with Tungsten Inert Gas (TIG) welding, presenting butt-welding with edge preparation in V. The crack is oriented parallel to the longitudinal axis of the weld and is consequently denominated as *toe crack* according to the quality standard [21].

The thermal analysis is performed with an IR (infrared) camera. The IR camera used for this work is NEC TH9260 with 640 × 480 Uncooled Focal Plane Array Detector (UFPA), with a resolution of 0.06°C and a measurement range from −40°C to 500°C. The camera is geometrically calibrated prior to data acquisition using a calibration grid based on the emissivity difference between the background and the targets, presented in [22]. The calibration parameters of the IR camera in the focus position used for data acquisition during the thermographic tests are shown in Table 1.

Finally, the photogrammetric process has been applied following the methodology established in [11]. For the implementation, a commercial digital single lens reflex (DSLR) camera, Canon EOS 500D, with a Sigma 50 mm macro lens is used. A tripod is used to stabilize the camera during acquisition due to the high exposure times required to get the correct lighting exposition. In order to homogenize and optimize the illumination conditions, two halogen lamps (50 W each) are also used.

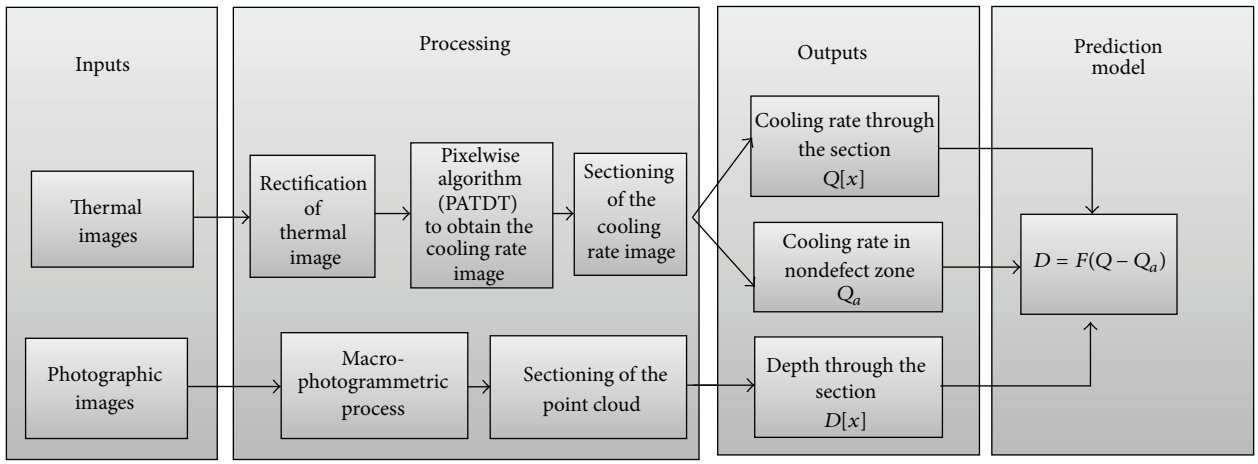

Figure 2: Methodology followed to obtain the prediction model. Inputs are the thermal and photographic images. Processing has two parts: the thermal procedure (firstly, the rectification of the image is implemented, after a PATDT algorithm is applied in order to obtain the cooling rate for each pixel of the image; subsequently, sectioning of the image through different lines is implemented in order to get discrete cooling rate functions) and the macrophotogrammetric procedure [10]. Finally, the processing of the inputs allows obtaining the cooling rates and depths through a concrete different section of the crack; with these outputs, a mathematical approach is applied in order to obtain the prediction model.

2.2. Methodology. The methodology applied for this research presents two different parts (Figure 2): on the one hand, a thermal processing is applied to extract the cooling rate for each pixel of the thermal matrix through two different sections; on the other hand, a photogrammetric procedure is applied to obtain the real depth values of the cracks through the two mentioned sections. The objective is to compare the two types of results in order to study the possible relation between them through a linear mathematical approach.

2.2.1. Thermal Data Procedure to Extract the Cooling Rates

(1) Acquisition of Thermal Images. The data acquisition protocol starts with the heating of the weld by a Joule effect heater until 40°C. The superficial temperature is controlled with a contact thermometer TESTO720 with Pt-100, resolution 0.1°C, and accuracy ±0.2°C. The thermometer is held on the surface of the plaque, in order to ensure total contact with the plaque and avoid the interference of the ambient conditions in the measurement. When the desired temperature is obtained, the heater is switched off and the IR camera is switched on. The monitoring of the cooling period is made with 50 thermograms, one every 5 seconds. Finally, the thermal images are extracted in RAW format, which implies one temperature value for each pixel, so that each image constitutes a matrix with the temperature values of the weld in the time of the acquisition.

(2) Rectification of Thermal Images. The objective of the rectification is to scale the thermal images to the real geometry, allowing the establishment of a correlation between temperature and depth values, the latest coming from the macrophotogrammetric procedure. If the thermal images have 2D metric, their different points can be related with the 3D metric dense point cloud obtained with macrophotogrammetry. The first step consists of the extraction of the temperature matrix of each thermographic image: each position in the matrix contains the temperature value of the corresponding part of the object contained in the image pixel. Values are corrected on an emissivity basis, using as reference the temperature values measured at the beginning of the test (prior heating) with the contact thermometer. The emissivity value is calculated using Stefan-Boltzmann's Law, and the correction is applied to the matrix for obtaining the real temperature values.

Once the temperature values are corrected, the infrared image matrix is subjected to a rectification algorithm. The core algorithm of image rectification is the plane projective transformation, ruled by

$$X = \Delta x + \frac{a_0 + a_1 x' + a_2 y'}{c_1 x' + c_2 y' + 1}$$
$$Y = \Delta y + \frac{b_0 + b_1 x' + b_2 y'}{c_1 x' + c_2 y' + 1}, \quad (1)$$

where X and Y are the rectified (real) coordinates of the element, x' and y' are the pixel coordinates in the image, and a_0, a_1, a_2, b_0, b_1, b_2, c_1, and c_2 are the mathematical coefficients of the projective matrix that enclose rotation, scale, translation, and perspective.

Therefore, the knowledge of the coordinates of 4 points in the object is the only requirement for the determination of the projective matrix, as well as the geometric calibration parameters of the camera ($\Delta x, \Delta y$).

(3) Pixelwise Algorithm for Time Derivative of Temperature (PATDT). Once images have been rectified, the next step is to apply an algorithm based on the approach developed in [21]. In this way, the cooling rate of the heated

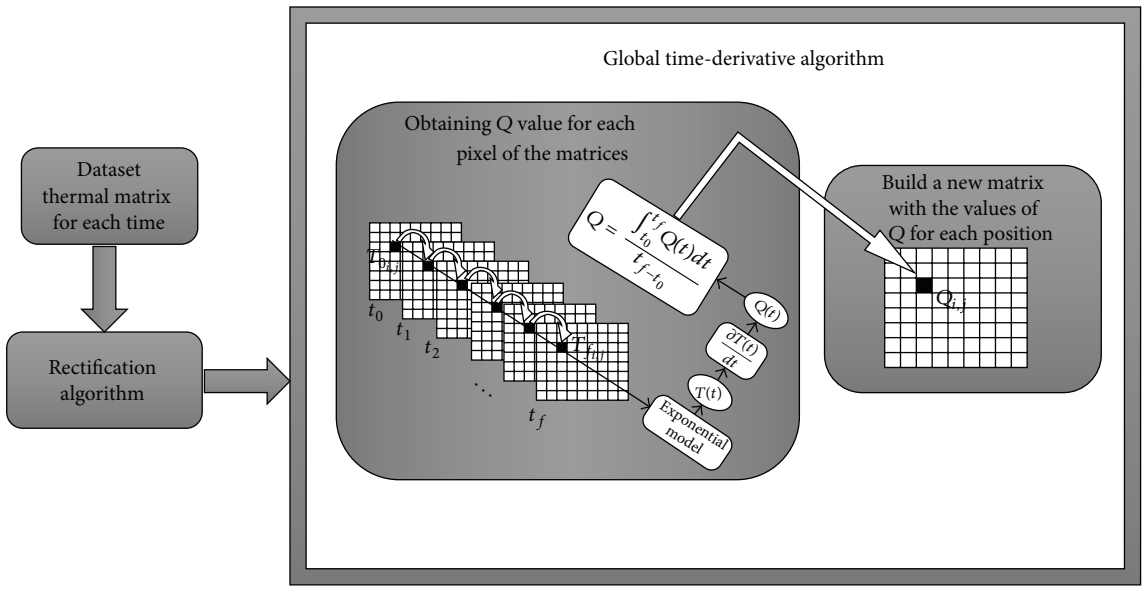

FIGURE 3: Steps followed by the global time-derivative algorithm. After data acquisition and rectification, the exponential model is applied for each (i, j) position with the values of temperature for each time instant. As a result, a temperature function is obtained and the time derivate of the temperature function is the cooling function, which is averaged for each position of the matrix, obtaining a matrix of cooling rates.

steel is analyzed according to Newton's Cooling Law. This law indicates that temperature decreases exponentially. This procedure based on the monitoring of the cooling allows the detection of defects without using complex processing algorithms (Figure 3), like those indicated in Section 1.

The PATDT applies Newton's Cooling Law for each pixel of the thermal image using an exponential fit model for the temperature-time data of each thermogram. Using this approach, a cooling rate function $Q(t)$ is established for each pixel as time derivate of the temperature function, $T(t)$. The sequence followed by the algorithm is the following (Figure 3):

(a) An exponential fit according to Newton Law is established for each temperature value $T_0, T_1, T_2, \ldots, T_j$, associated with each time instant $t_0, t_1, t_2, \ldots, t_f$ and for each pixel position of matrix, obtaining an expression $T(t)$ for each pixel position.

(b) The derivation $\partial T(t)/dt$ is calculated in order to obtain the cooling rate function $Q(t)$ for each pixel position.

(c) An integrated average Q for $Q(t)$ between the initial and final time is calculated for each pixel position.

A new matrix with the same dimensions as the thermal matrix is created. The integrated average cooling rate $Q_{i,j}$ is introduced on each i, j position of the matrix obtaining a cooling rate matrix.

In order to work with relative cooling rate data, each cooling rate value corresponding to the crack (Q_{ij}) is subtracted from the average of immediate exterior pixels Q_a *from a 10-pixel zone placed immediately near the crack*. In this way, the relative cooling rate is obtained for each pixel of the crack and a relative cooling rate matrix is obtained as $Q_{ij} - Q_a$, being i, j the dimensions of the crack submatrix.

2.2.2. Macrophotogrammetric Procedure to Extract Depth Data. The generation of the photogrammetric 3D model of the crack is done following the procedure established in detail by the authors in [11]. The first step is the acquisition of photographic images with a DSLR camera following a semispherical trajectory centered on the object. Once images are acquired, keeping always a constant distance between the lens and the object, two processing steps are applied: first, the automatic determination of the spatial and angular positions of each image, regardless of the order of acquisition and without requiring initial approximations or camera calibration, and second, the automatic computation of a dense 3D point cloud (submillimetric resolution), so that each pixel of the image renders a specific point of the model of the weld (Figure 4).

2.2.3. Correlation between Cooling Rate and Depth Data for Each Section for the Generation of the Model and Validation. When the cooling rate function for each section is obtained following the thermal procedure established in Section 2.2.1 and the depth function for each section is extracted following the macrophotogrammetric procedure explained in Section 2.2.2, the correlation between the points of both functions is established for every two different longitudinal sections in order to design a mathematical lineal model that allows the crack-depth prediction based on the cooling rate (Figure 2). Two transversal sections are used for the external validation of the model. Additionally, the method is applied to other cracks in other welds in order to establish an external validation of the method (Figure 4).

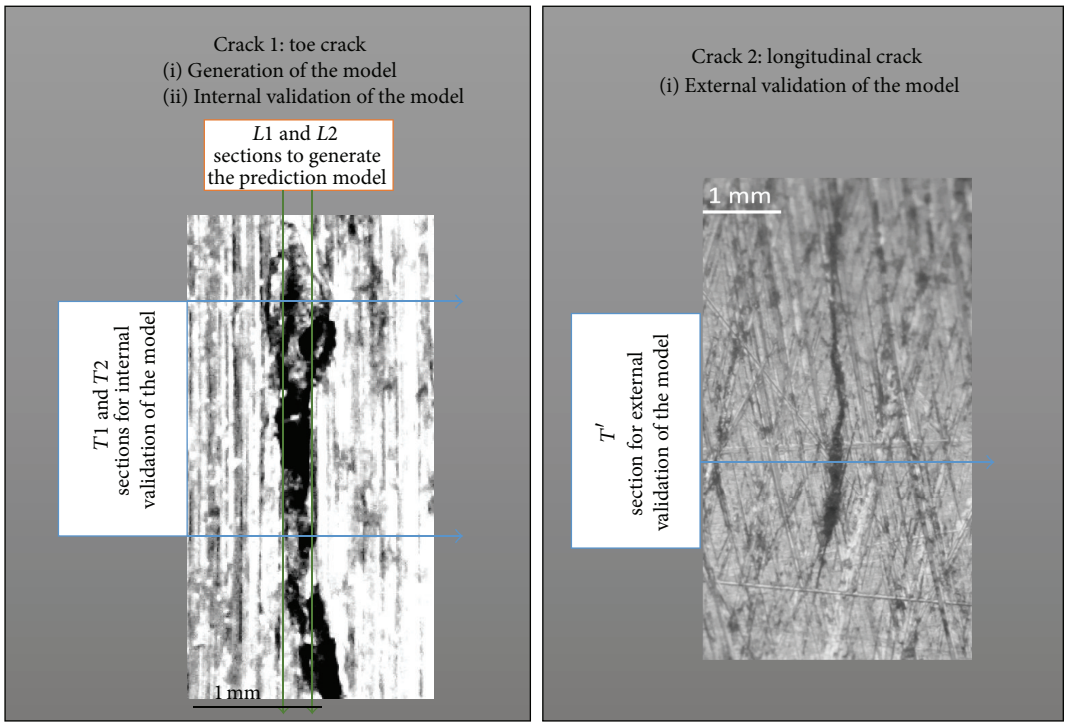

Figure 4: Cracks with sections used to generate the model ($L1$ and $L2$), internal validation ($T1$ and $T2$), and external validation (T').

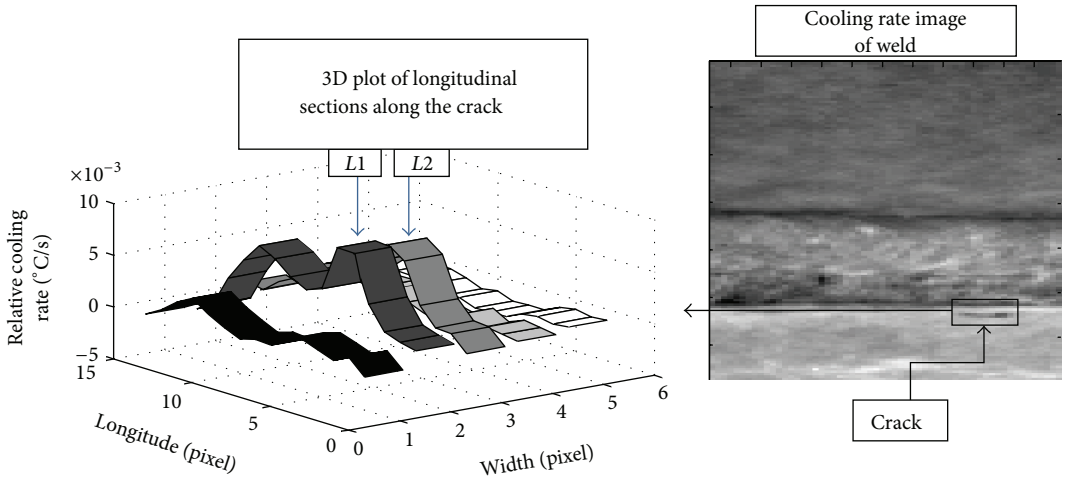

Figure 5: 3D representation of the crack zone based on the relative cooling rate matrix obtained following the procedure illustrated by Figure 3. In Figure 6, the two pixel rows of the crack ($L1$ and $L2$) are labeled.

3. Results

3.1. Cooling Rate Results. The graphical representation of the relative cooling rate matrix segmented in the crack region in 3D is shown in Figure 6. The average cooling rate for the adjacent zone to the defect, Q_a, is 0.0149°C/s. The cooling rate through two sections ($L1$ and $L2$) is studied in Figure 6.

3.2. Depth Results. The macrophotogrammetric model for the crack is obtained from the matching of images, which are acquired from convergent positions with respect to the weld, repeating the procedure exposed in [11].

For the computation of depths, the point cloud from the macrophotogrammetric procedure is sectioned in the two longitudinal sections ($L1$ and $L2$) (Figure 4). The section of the point cloud with normal planes $L1$ and $L2$ is applied in order to extract the depth for each pixel (Figure 5). The metrical reference between depths on the dense point cloud and the cooling rate values is made using the distances from the extremes of the crack.

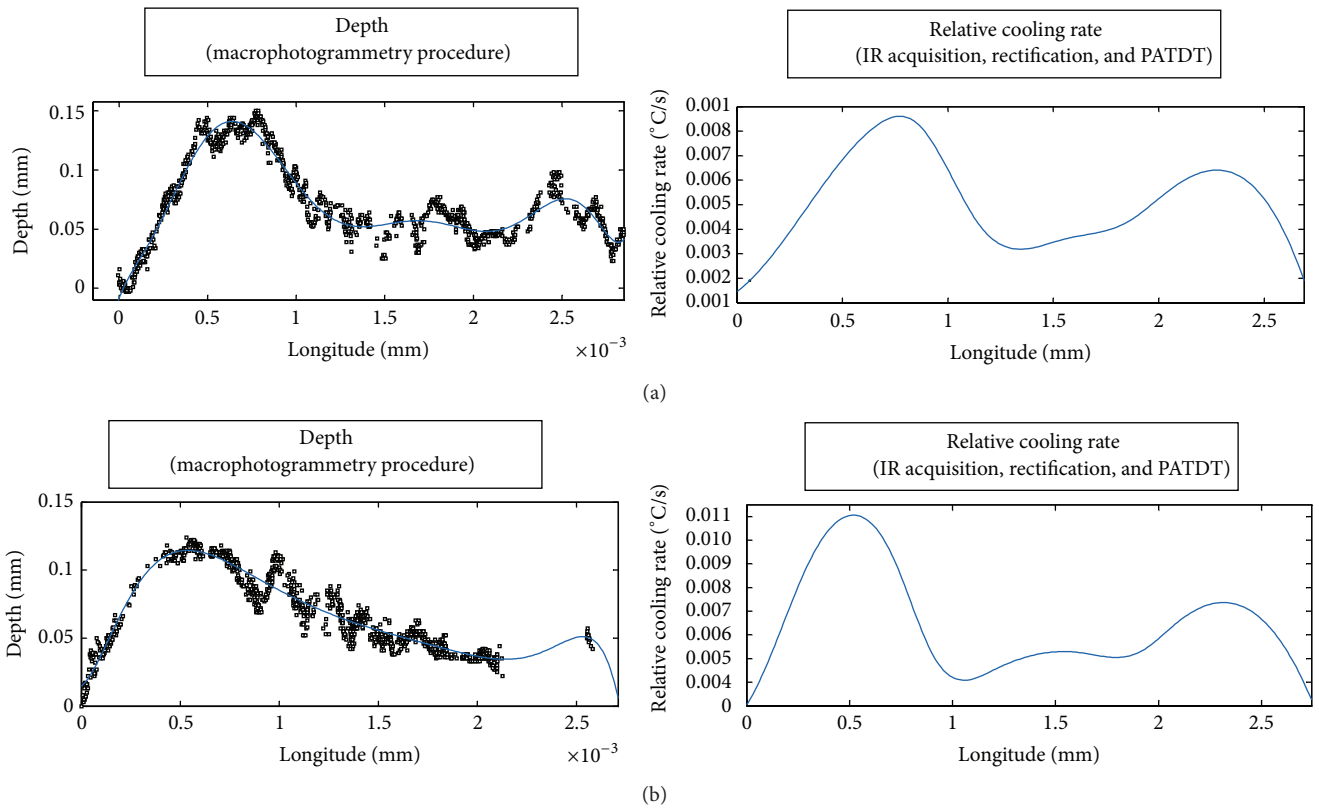

Figure 6: Depth function and relative cooling rate function along the longitudinal sections ($L1$ (a) and $L2$ (b)).

The fit is used because the number of points is higher than the number of pixels on the cooling rate image. For this reason, authors have chosen to work with continuous functions in order to ease the correlation of data. The fit model used to obtain a depth function that allows the estimation of the real depth is a 9-degree polynomial fit, which provides an acceptable goodness (Root Mean Square Error (RMSE) of 0.0098 for longitudinal section $L1$ and RMSE of 0.0082 for longitudinal section $L2$).

3.3. Correlation between Cooling and Depth Data. When relative cooling rate and depth data have been obtained through each section (Figure 6), each pair of values (depth-relative cooling rate) is extracted from 20 longitude values and correlated in order to establish a prediction model which allows the estimation of the depth using just the cooling rate value.

The correlation between depth and relative cooling rate $(Q - Q_a)$ (Figure 7) is obtained with a fitting error of 0.86 (Table 2). For this reason, the prediction model is considered as acceptable, which demonstrates the existence of a coherent mathematical relationship between depth (mm) and cooling rate (°C/s).

Table 2: Parameters of the lineal fit which correlates relative cooling rate and depth.

$D = a(Q - Q_a) + b$		
Gain (a)	Offset (b)	R^2
15.71	−0.002534	0.857

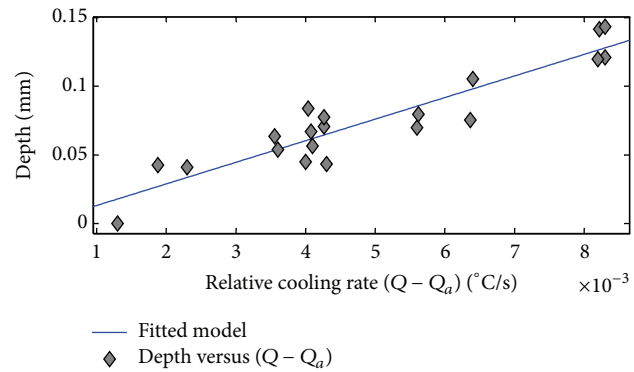

Figure 7: Correlation between depth and relative cooling rate for each pixel in the crack.

4. Validation

4.1. Internal Validation of the Prediction Model. In order to test the validity of the model, an internal validation procedure is applied through the analysis of two transversal sections ($T1$ and $T2$) in the same crack (Figure 4). These sections are performed in a direction where the difference of depth between positions is the highest. The aim of this step is

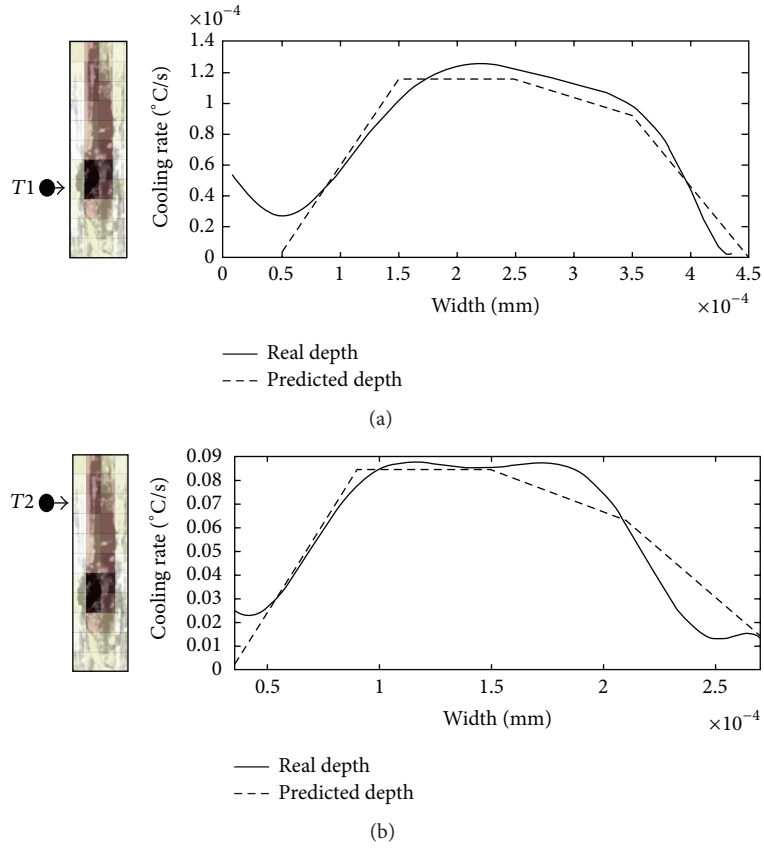

FIGURE 8: Transversal sections used for the internal validation of the model ($T1$ (a) and $T2$ (b)).

to analyze the correspondence between the predicted depth values $P[x]$ (where x is the width) calculated with the prediction model (Table 2) from the cooling rate data with the real depth values $V[x]$ extracted from the sectioning of the point cloud. These sections are significantly smaller than the longitudinal sections used to build the prediction model (Figure 4) but present a higher contrast of the cooling rate. For this reason, the application of the prediction model to those points belonging to these transversal sections serves to analyze the internal coherence of the model and thus the goodness of the fit.

The prediction model is applied to each transversal section (Figure 8). Then, the prediction model is compared with the real model in order to analyze the accuracy. The error is calculated for each x value with the following discrete expression:

$$\varepsilon = \sum_{x_0}^{x_f} |V[x] - P[x]|, \quad (2)$$

where V is the real value of depth and P is the predictive value (both for the same value of x). The error of the prediction model for the first transversal section, $T1$ (Figure 8), is 0.00169 mm (14%) and the error for the second transversal section, $T2$, is 0.0010 mm (13%).

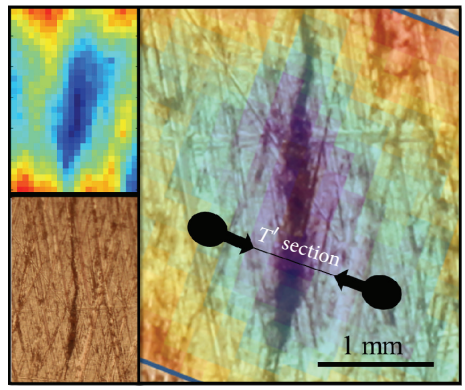

FIGURE 9: Cooling rate matrix of the new crack, with pseudocolor assigned to each cooling rate value (top left) and macrophotography of the crack (bottom left). Overlapping of cooling rate map with macrophotography of the crack in order to correlate the different depths of the crack with the different cooling rate data (right). The transversal section T' used to assess the prediction model has been plotted.

4.2. External Validation of the Prediction Model. In this section, the robustness of the prediction model is tested through its application to the estimation of the depth in a crack open to surface in a different plate, made of the same material (Figure 9). In this case, the crack is a longitudinal

crack open to surface placed on the weld (weld cap removed) and generated by the stress provoked during the welding process. This crack is significantly smaller (tenths of mm) than the crack used to build the model, which is the reason for its choice. In this way, authors seek to test the model under stringent requirements.

The macrophotogrammetric procedure is repeated for this new crack in order to obtain accurately the depth distribution of the crack (denominated as *real depth*). Then, the plate is heated at 70°C. This temperature, higher than in the previous case, is necessary in order to obtain a correct visualization of the crack in the thermal matrix, given the small size of this crack. The cooling period is monitored for 250 s (the same period). The cooling rate is calculated from the thermal images for each time instant following the procedure established in Section 2.2.1(3). Subsequently, the average cooling rate for the adjacent zone of the crack, Q_a, is calculated. The result is 0.0516°C/s. Then, the prediction model calculated in Section 3.3 is applied through the values of transversal section of the crack (called section T') and the depth values are estimated for each pixel from the cooling rate data (Figure 9).

At this point, real and prediction models are compared in order to analyze the error of the predicted model regarding the reality. Both models are shown in Figure 10. The resulting error of the prediction model is 0.009 mm (18%). This result is acceptable knowing that the maximum depth in the crack is 0.05 mm.

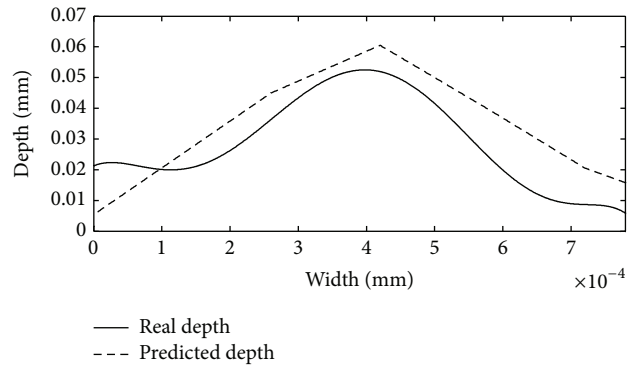

Figure 10: Real and predicted depth through the transversal section T' used for the external validation of the model.

5. Conclusions

A procedure for the prediction of depth of cracks from infrared data has been implemented. This approach represents a methodological innovation in the field of Nondestructive Testing for the evaluation of weld flaws.

The procedure applied allows the accurate prediction of different depths of the crack from thermal images. Low-temperature heating (40°) is applied to the steel and the cooling is monitored for 250 s. Although the heat transfer tends to be homogenized through the material in long cooling times, the values of the cooling rate also depend on the surface properties for each point of the material. Therefore, different surface properties in the defect and the nondefect zone provide a difference in the heat dissipation which provokes a difference in the cooling rates. This difference is clearly visible for each pixel through the sections of thermal images. These thermal data are associated with the real depths obtained with a reliable and experienced macrophotogrammetric procedure [10] using a commercial DSLR camera.

The cooling rate value for each pixel is different for each time moment, since the cooling rate is higher at the beginning of the cooling process than at its end due to the exponential reduction of the temperature. The registration and integration of the cooling rate values from 250-second cooling interval allows the registration of the totality of information. For this reason, the homogenization of the heat transfer through the material is not a limit for the methodology, since results present enough contrast to establish a depth prediction model.

The prediction model established through the correlation between cooling rate and depth maintains statistical consistency allowing an acceptable fit (RMSE between 0.008 and 0.009). Furthermore, the prediction model has been validated following a twofold approach: on the one hand, an internal validation has been implemented, consisting of the application of the prediction model to the crack in two transversal sections (different sections to those used to obtain the prediction model). These transversal sections have been chosen since they present high thermal contrast in a minimal space, subjecting the prediction model to a limit situation. Results demonstrate the good precision of the method to predict depth values of cracks, with 15% of maximum deviation. On the other hand, an external validation has been applied through the analysis of a different crack. In this case, a crack open to surface located in cap removing weld has been used to provide the external validation. With this test, authors analyze not only the validity of the method for other cracks, but also the quality of the prediction model when the heating is done at different temperatures (in this case, higher, 70°C). Results of the prediction model are consistent, with 18% of maximum deviation regarding real depth. The error is mainly due to the interpolation method used for the relation of thermal and depth values. It could be improved using more discrete values and this is a future goal that this work opens.

The procedure has been applied to cracks generated from the stress provoked by the welding process in low-carbon steel. However, the procedure could be extended to the analysis of cracks in other materials. The cooling phenomenon is studied by the Newton Law and depends on the physical property of the materials as conductivity, heat capacity, surface features, and so forth. For this reason, the extension of the technique to other materials will be researched in future works.

Conflict of Interests

The authors declare that there is no conflict of interests regarding the publication of this paper.

Acknowledgment

The authors would like to thank Agencia de Innovación y Financiación Empresarial de Castilla y León (ADE), Ministerio de Economía y Competitividad (Gobierno de España), for the financial support given through human resources grants (FPDI-2013-17516).

References

[1] ISO, "Welding. Fusion-welded joints in steel, nickel, titanium and their alloys (beam welding excluded). Quality levels for imperfection," ISO 5817:2009, European Committee for Standardization, 2009.

[2] T. W. Liao, "Classification of weld flaws with imbalanced class data," *Expert Systems with Applications*, vol. 35, no. 3, pp. 1041–1052, 2008.

[3] IAB, "Minimum Requirements for the Education, Examination and Qualification," Tech. Rep. 252r2-14/SV-00, IAB—International Authorization Board, 2014.

[4] BS, "Guide to methods for assessing the acceptability of flaws in metallic structures," Tech. Rep. BT7910:2013, The British Standards Institution, 2013.

[5] M. V. Felice, A. Velichko, and P. D. Wilcox, "Accurate depth measurement of small surface-breaking cracks using an ultrasonic array post-processing technique," *NDT & E International*, vol. 68, pp. 105–112, 2014.

[6] H.-S. Huang, "Fracture characteristics analysis of pressured pipeline with crack using boundary element method," *Advances in Materials Science and Engineering*, vol. 2015, Article ID 508630, 13 pages, 2015.

[7] E. Maire, J.-Y. Buffière, L. Salvo, J. J. Blandin, W. Ludwig, and J. M. Létang, "On the application of X-ray microtomography in the field of materials science," *Advanced Engineering Materials*, vol. 3, no. 8, pp. 539–546, 2001.

[8] S. Henkel, D. Holländer, M. Wünsche et al., "Crack observation methods, their application and simulation of curved fatigue crack growth," *Engineering Fracture Mechanics*, vol. 77, no. 11, pp. 2077–2090, 2010.

[9] L. Zhang, W. Ke, Q. Ye, and J. Jiao, "A novel laser vision sensor for weld line detection on wall-climbing robot," *Optics and Laser Technology*, vol. 60, pp. 69–79, 2014.

[10] M. Dinham and G. Fang, "Autonomous weld seam identification and localisation using eye-in-hand stereo vision for robotic arc welding," *Robotics and Computer-Integrated Manufacturing*, vol. 29, no. 5, pp. 288–301, 2013.

[11] M. Rodríguez-Martín, S. Lagüela, D. González-Aguilera, and P. Rodríguez-Gonzálvez, "Procedure for quality inspection of welds based on macro-photogrammetric three-dimensional reconstruction," *Optics & Laser Technology*, vol. 73, pp. 54–62, 2015.

[12] M. Rodríguez-Martín, S. Lagüela, D. González-Aguilera, and J. Martinez, "Prediction of depth model for cracks in steel using infrared thermography," *Infrared Physics & Technology*, vol. 71, pp. 492–500, 2015.

[13] R. Frappier, A. Benoit, P. Paillard, T. Baudin, R. Le Gall, and T. Dupuy, "Quantitative infrared analysis of welding processes: temperature measurement during RSW and CMT-MIG welding," *Science and Technology of Welding and Joining*, vol. 19, no. 1, pp. 38–43, 2014.

[14] S. Nagaraju, A. Rajadurai, M. Vasudevan, M. Menaka, and R. Subbaratnam, "Novel method for quantitative assessment of slag detachability in austenitic stainless steels welds made by SMAW," *Science and Technology of Welding and Joining*, vol. 13, no. 8, pp. 739–743, 2008.

[15] X. Maldague, F. Galmiche, and A. Ziadi, "Advances in pulsed phase thermography," *Infrared Physics & Technology*, vol. 43, no. 3–5, pp. 175–181, 2002.

[16] G. Busse, A. Gleiter, and C. Spiessberger, "NDE using lockin-thermography: principle and recent developments," in *Nondestructive Testing of Materials and Structures*, vol. 6 of *RILEM Bookseries*, pp. 627–632, Springer, Dordrecht, The Netherlands, 2013.

[17] A. Castelo, A. Mendioroz, R. Celorrio, and A. Salazar, "Vertical cracks characterization and resolution from lock-in vibrothermography," in *Proceedings of the 12 International Conference on Quantitative Infrared Thermography*, Bordeaux, France, July 2014.

[18] A. Mendioroz, A. Castelo, R. Celorrio, and A. Salazar, "Characterization and spatial resolution of cracks using lock-in vibrothermography," *NDT & E International*, vol. 66, pp. 8–15, 2014.

[19] D. Palumbo, F. Ancona, and U. Galietti, "Quantitative damage evaluation of composite materials with microwave thermographic technique: feasibility and new data analysis," *Meccanica*, vol. 50, no. 2, pp. 443–459, 2014.

[20] M. Rodríguez-Martín, S. Lagüela, D. González-Aguilera, and P. Arias, "Cooling analysis of welded materials for crack detection using infrared thermography," *Infrared Physics and Technology*, vol. 67, pp. 547–554, 2014.

[21] ISO, "Welding and allied processes—classification of geometric imperfections in metallic materials—part 1: fusion welding," EN-ISO 6520-1:2009, European Committee for Standardization, 2009.

[22] S. Lagüela, H. González-Jorge, J. Armesto, and J. Herráez, "High performance grid for the metric calibration of thermographic cameras," *Measurement Science and Technology*, vol. 23, no. 1, Article ID 015402, 2012.